[*Reprinted from* THE AERONAUTICAL JOURNAL OF THE ROYAL AERONAUTICAL SOCIETY, *MAY 1994*]

A cavitating aerofoil with a Prandtl–Batchelor eddy

E. ZACHARIOU and P. WILMOTT
Mathematical Institute
Oxford

and

A. D. FITT
Faculty of Mathematical Studies
University of Southampton

PRINTED BY MANOR PARK PRESS LIMITED. EDISON ROAD. HAMPDEN PARK EASTBOURNE. SUSSEX ENGLAND
AND PUBLISHED BY THE ROYAL AERONAUTICAL SOCIETY 4 HAMILTON PLACE. LONDON W1V 0BQ. ENGLAND

A cavitating aerofoil with a Prandtl–Batchelor eddy

E. ZACHARIOU and P. WILMOTT
Mathematical Institute
Oxford

and

A. D. FITT
Faculty of Mathematical Studies
University of Southampton

ABSTRACT

A simple model is presented for an aerofoil with a recirculating Prandtl-Batchelor region behind a spoiler. Using thin aerofoil theory the model is posed as a pair of coupled nonlinear singular integrodifferential equations for the shape of the separating streamline and the distribution of vorticity along the aerofoil. These equations are solved numerically and results are presented. In particular, some conclusions are drawn regarding the lift on such aerofoils.

NOMENCLATURE

C_L	lift coefficient
$h(x)$	shape of aerofoil
L	lift
L_a	aerofoil length
n_α	mesh point number when $x = \alpha$
n_β	mesh point number when $x = \beta$
N	total number of mesh points
p_∞	freestream pressure
$S(x)$	shape of cavity
U_∞	freestream velocity
v	slope of spoiler
$v(x)$	vorticity distribution
x	horizontal coordinate
y	vertical coordinate
Y	scaled vertical coordinate in cavity
α	end of spoiler
β	position of cavity reattachment
Γ	non-dimensional vorticity
ε	slenderness parameter
κ	Bernoulli constant
λ	scaled perturbation to Bernoulli constant
μ	slope of aerofoil
ρ	density
$\sigma(x)$	source distribution
ψ	stream function
Ψ	scaled stream function

Superscripts

$\bar{}$	perturbation quantity
$*$	non-dimensional quantity

Paper received 18 April 1993, revised version received 29 September 1993
Accepted 31 March 1994.
Paper No. 1947

1. INTRODUCTION

A simple model for a stalled aerofoil is presented. In the present context, the word "stalled" does not imply that the angle of attack of the aerofoil is large, for thin aerofoil theory will be applied, but rather that the aerofoil possesses an eddy located on its top surface. Some details of the geometry are given in Fig. 1. Observe that separation is ensured by the addition of a spoiler with a sharp corner. From this corner a separating streamline emerges which, provided the eddy is not too long, reattaches tangentially further downstream on the top surface of the aerofoil. Within the region enclosed by the streamline and aerofoil/spoiler the existence of a Prandtl-Batchelor[1] zone of constant vorticity is assumed. Elsewhere the flow is assumed irrotational. If the body/eddy combination is sufficiently slender then thin aerofoil theory may be applied; we adopt this approach here as it leads to a number of productive simplifications. Historically, aerofoils where the flow is separated have proved notoriously difficult to model. It is important, however, that simplified models are developed, both for the purposes of calibration of highly complicated three-dimensional numerical models and to offer conceptual understanding. Before describing the model in detail some relevant work of importance is discussed.

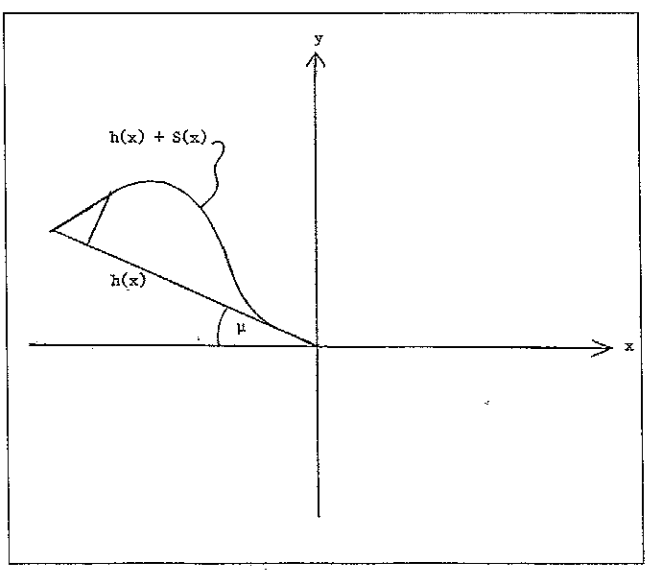

Figure 1 Geometry for aerofoil/spoiler combination

Other constant eddy models have been used with success by Childress[2] and O'Malley *et al*[3]. Childress models the separated flow behind both wedges and backward-facing steps by a Prandtl-Batchelor region, and O'Malley *et al* extend this idea by including both a Prandtl-Batchelor region and a region of constant pressure (the classical Helmholtz-Kirchhoff model) The idea of a Helmholtz-Kirchhoff (i.e. constant pressure) infinite cavity has been applied to aerofoils by Woods[4] (see also Ockendon & Tayler[5]) In the Childress model the free boundary value problem can be reduced to a nonlinear integral equation for the shape of the boundary between the eddy and the irrotational part of the flow. This model is adopted below with the result that the shape of the separating streamline and the vorticity distribution are determined by two coupled nonlinear singular integrodifferential equations (Section 2) The numerical solution of these equations is discussed in Section 3 and results and conclusions are presented in section 4.

2. THE CAVITATING AEROFOIL

Guided by the Childress model for high Reynolds number flow over a backward facing step, a model of a thin aerofoil with a spoiler in the shape of a backward facing step attached to the top surface at the leading edge is considered, as shown in Fig. 1 The model for the flow will be derived for an arbitrarily shaped aerofoil. Specific examples and special cases will be considered in later sections.

Referring again to Fig. 1, the region outside the aerofoil/cavity body will be termed the "outer region" Under the assumption of inviscid, incompressible, irrotational flow with undisturbed free stream speed U_∞ and density ρ, the stream function ψ in the outer region must satisfy

$$\nabla^2\psi = 0$$

with

$$\psi \sim U_\infty y \quad \text{as} \quad y \to \infty$$

In addition, there must be no normal flow on the surface of the aerofoil/spoiler body, and the Kutta condition of tangential flow at the trailing edge of the aerofoil must be satisfied. As shown in Fig 1 the shape of the bottom surface of the aerofoil is given by $y = h(x)$, (the aerofoil is assumed to have zero thickness and $h(x)$ therefore represents both the upper and the lower surface of the aerofoil) whilst the shape of the top surface is given by $y = S(x)+h(x)$. The aerofoil has length L, and p_∞ is the pressure in the free stream far away from the body. The model is non-dimensionalised with

$$\psi = U_\infty L\psi^*$$
$$x = Lx^*$$
$$p = \frac{1}{2}\rho U_\infty^2 p^* + p_\infty$$
$$h = \varepsilon L h^*$$
$$S = \varepsilon L S^*$$

Here ε is a small parameter which is defined more carefully below, but reflects the fact that the aerofoil is slender, and is assumed to be the same order of magnitude as the angle of incidence of the aerofoil to the freestream. Dropping the stars for convenience, we therefore seek a solution of the form

$$\psi = y + \varepsilon\bar{\psi}$$

where $\bar{\psi}$ is to be determined.

The stream function $\bar{\psi}$ is represented by unknown distributions of sources and vorticity and a solution is sought of the form

$$\bar{\psi} = \int_0^1 \sigma(t)\tan^{-1}\left(\frac{y}{x-t}\right)dt + \int_0^1 \nu(t)\log((x-t)^2+y^2)dt \qquad (1)$$

where σ and ν are to be determined.

From the work of Batchelor[1] it is known that if a steady planar flow of an inviscid incompressible fluid contains one or more regions within which the streamlines are closed, then in those regions the flow has uniform vorticity In the "inner" region of separated flow, the non-dimensional stream function ψ therefore satisfies

$$\nabla^2\psi = -\Gamma$$

with $\psi = 0$ on the boundaries. The order of magnitude of Γ, the non-dimensional vorticity, is still to be determined. The recirculating region is separated from the main flow and hence across the streamline $y = \varepsilon(S(x)+h(x))$ there will, in general, be a jump in the Bernoulli constant. Note also that $S(x)$ is partly known since upstream of the recirculating region the geometry of the spoiler is prescribed, whilst after reattachment $S(x)$ is simply equal to $h(x)$. Above the recirculating region, however, S is to be determined.

2.1 The outer flow

In the outer region the problem for $\bar{\psi}$ is

$$\nabla^2\bar{\psi} = 0$$

with, to lowest order

$$-\bar{\psi}_x = h_x + S_x \quad \text{on} \quad y = 0_+$$

and

$$-\bar{\psi}_x = h_x \quad \text{on} \quad y = 0_-$$

As per traditional thin aerofoil theory, the boundary conditions have been imposed not on the free surface itself, but on a slit on the x-axis As $y \to 0$ we find from equation 1 that, for $x \in [0, 1]$

$$\bar{\psi}_x = -\pi\sigma(x)\,\mathrm{sgn}y + 2\int_0^1 \frac{\nu(t)}{x-t}dt$$

where the bar through the integral sign denotes the Cauchy principal value in the normal way. Imposing the boundary conditions on y = 0+ and y = 0– now gives

$$\sigma(x) = \frac{S'}{2\pi} \qquad (2)$$

and

$$\int_0^1 \frac{\nu(t)}{x-t}\,dt = -\frac{h'}{2} - \frac{S'}{4} \qquad (3)$$

Another well-known result from thin aerofoil theory states that in order for the Kutta condition to be satisfied $\nu(1) = 0$ The non-dimensional pressure in the outer region may now be determined. We have

$$p + \frac{1}{2}|\nabla\psi|^2 = \frac{p_\infty}{\rho U_\infty^2} + \frac{1}{2}$$

and on using Equations (1) and (2) and setting $y = 0+$ we find that

$$p = \frac{p_\infty}{\rho U_\infty^2} - \frac{\varepsilon}{2\pi}\int_0^\beta \frac{S'(t)}{x-t}dt - 2\varepsilon\pi\nu(x)$$

2.2 The cavity flow

In the inner region it is appropriate to rescale the y variable by setting $y = \varepsilon Y$ To leading order we find that

$$\psi_{YY} = -\varepsilon^2 \Gamma$$

with

$$\psi = 0 \quad \text{on} \quad Y = h \quad \text{and} \quad Y = h + S$$

giving

$$\frac{\psi}{\varepsilon^2} = -\frac{1}{2}\Gamma Y^2 + \frac{1}{2}Y\Gamma(S+2h) - \frac{1}{2}h\Gamma(S+h)$$

On $Y = S + h$ in the inner region we have, from Bernoulli

$$p + \frac{1}{2}|\nabla\psi|^2 = \kappa$$

where κ is the Bernoulli constant. Thus to leading order

$$p = \kappa - \frac{1}{8}(\Gamma S)^2\varepsilon^2 \tag{4}$$

For this to be consistent with an order ε perturbation to the outer pressure we require $\Gamma = O(\varepsilon^{-1/2})$ so that $\Psi = O(\varepsilon^{3/2})$. Writing $\Gamma = \varepsilon^{-1/2}\bar{\Gamma}$ and dropping the overbar, the pressures may be matched to yield an integral equation for $S'(x)$ We assume also that the downstream tip of the spoiler is at $x = \alpha$, while reattachment takes place at $x = \beta$. This gives

$$\kappa - \frac{\varepsilon}{8}(\Gamma S)^2 = \frac{p_\infty}{\rho U_\infty^2} - \frac{\varepsilon}{2\pi}\int_0^\beta \frac{S'(t)}{x-t}dt - 2\varepsilon\pi\ \nu(x)$$

Further setting

$$\kappa = \frac{p_\infty}{\rho U_\infty^2} + \lambda\varepsilon$$

the two equations which determine $\nu(x)$ and $S(x)$ are (3) and, for $x \in [\alpha, \beta]$,

$$\lambda - \frac{(\Gamma S)^2}{8} = -\frac{1}{2\pi}\int_0^\beta \frac{S'(t)}{x-t}\,dt - 2\pi\nu(x) \tag{5}$$

The relevant boundary conditions are that at $x = \alpha$ the streamline leaves the spoiler smoothly, whilst reattachment at $x = \beta$ is tangential. Thus

$$S(\alpha+) = S(\alpha-),\ S'(\alpha+) = S'(\alpha-)$$

and

$$S(\beta) = S'(\beta) = 0$$

It should be noted that for the symmetric version of the model $\nu = 0$ and equation (5) agrees with Ref 2.

2.3 Analysis of the model

To simplify the geometry we shall assume that the aerofoil/spoiler combination takes the form of a flat plate aerofoil with an attached triangular wedge beginning at the leading edge Thus

$$h' = \mu$$

where μ is a constant which will be less than zero for aerofoils with positive angles of attack. In this case we have

$$\int_0^\beta \frac{S'(t)}{x-t}dt = -\nu\log\frac{x-\alpha}{x} + \int_\alpha^\beta \frac{S'(t)}{x-t}dt$$

where ν is the (constant) slope of S in the region $[0, \alpha]$.

The two integral equations and boundary conditions now become

$$\frac{1}{2\pi}\int_\alpha^\beta \frac{S'(t)}{x-t}dt = -\lambda + \frac{\Gamma^2}{8}S^2 + \frac{1}{2\pi}\nu\log\left(\frac{x-\alpha}{x}\right) - 2\pi\nu(x) \qquad (x \in [\alpha,\beta]) \tag{6}$$

with

$$S(\alpha) = \nu\alpha,\quad S'(\alpha) = \nu,\quad S(\beta) = S'(\beta) = 0$$

and

$$\int_0^1 \frac{\nu(t)}{x-t}dt = -\frac{\mu}{2} - \frac{S'}{4} \qquad (x \in [0,1]) \qquad \text{with } \nu(1) = 0 \tag{7}$$

Once these equations have been solved the stream function and pressure of the flow may be calculated. Also, by the Kutta-Joukowski theorem, the lift L_a associated with the aerofoil and cavity may be calculated

Some discussion is required concerning the number of free parameters in the model. In reference 2 (corresponding to the case $\nu = 0$ in the present study) it was found that, once the reattachment point β was specified, the quantities λ and Γ were uniquely determined. The same is true of the more general problem defined by (6) and (7). The easiest way to obtain relationships between λ and Γ is to multiply (6) by suitable functions and integrate from α to β. For example, multiplying both sides of (6) by $S'(x)$ and integrating, we find that

$$\frac{\nu}{2\pi}\int_\alpha^\beta S'(x)\log\left(\frac{x-\alpha}{x}\right)dx + \lambda S(\alpha) - \frac{\Gamma^2}{24}S^3(\alpha) - 2\pi\int_\alpha^\beta \nu(x)S'(x)dx = 0 \tag{8}$$

a relationship similar to that found by Childress. For the case of flow over a backward-facing step when $\nu = 0$ and there is no logarithmic term in the expression above, a very simple relationship between λ and Γ results. In the next section we show that, as far as the numerical analysis of the problem is concerned, there are more convenient relationships than (8), but the crucial point is that each relationship of this sort may be thought of as a compatibility condition corresponding to the correct prescription of the slope of $S(x)$ at one or other of the end points Consequently there are only two such independent relationships.

3. Numerical solution of the equations

The equations and boundary conditions (6) and (7) constitute a system of coupled nonlinear singular integrodifferential equations for the functions ν and S, and the literature does not contain any simple numerical schemes for such equations. Further, the essential nonlinearity of the problem and the nature of the half-range Hilbert transform operator make it unlikely that practical results concerning convergence etc. will be available for any numerical method which might be used. We therefore proceed in an *ad hoc* manner, solving (6) and (7) by direct iteration. Before this may be accomplished, some manipulation is necessary as it is evidently desirable to avoid the numerically awkward operations of numerical differentiation and Hilbert transform evaluation wherever possible. With these considerations in mind, we begin by inverting equation (6) to yield

$$S'(x) = \frac{(\beta-x)^{1/2}}{\pi(x-\alpha)^{1/2}}\int_\alpha^\beta \frac{(t-\alpha)^{1/2}f(t)}{(\beta-t)^{1/2}}\frac{dt}{t-x} + \frac{A}{((\beta-x)(x-\alpha))^{1/2}}$$

where

$$f(t) = -2\lambda + \frac{\Gamma^2}{4}S^2 + \frac{\nu}{\pi}\log\left(\frac{x-\alpha}{x}\right) - 4\pi\nu(x)$$

The coefficient A of the eigenfunction is zero since $S'(\beta) = 0$, and on integrating with respect to x and choosing the constant of integration to be zero so that $S(\beta) = 0$ we find that, for $\alpha \le x \le \beta$

$$S(x) = \left(-\frac{2}{\pi}\sqrt{\frac{\beta - x}{\beta - \alpha}} \right) \int_\alpha^\beta \sqrt{\frac{t-\alpha}{\beta - t}} f(t)dt +$$

$$\frac{1}{\pi}\int_\alpha^\beta f(t) \log\left(\frac{\left(\sqrt{(\beta - t)(x-\alpha)} + \sqrt{(\beta - x)(t-\alpha)}\right)^2}{(\beta-\alpha)|x-t|} \right) dt \qquad (9)$$

For numerical purposes, equation (9) is in a convenient form as the integrals are no longer of Cauchy principal value type and derivatives of S do not appear Further, the quantities Γ and λ may be eliminated from (9) by utilising compatibility conditions as described in the previous section. The most convenient way of accomplishing this is to multiply by $((x - \alpha)/(\beta - x))^{\pm 1/2}$ and integrate with respect to x from α to β. The two equations for Γ^2 and λ which result may be solved to yield

$$\Gamma^2 = \frac{8(\nu\alpha + J_5 + J_6 - J_2 - J_3)}{J_1 - J_4} \qquad (10)$$

$$\lambda = \frac{\nu\alpha(J_1 + J_4) + 2(J_1 J_6 + J_1 J_5 - J_4 J_5 - J_2 J_4)}{\pi(\beta - \alpha)(J_1 - J_4)} \qquad (11)$$

where

$$J_1 = \int_\alpha^\beta \sqrt{\frac{\beta - x}{x - \alpha}} S^2(x)dx \qquad J_2 = \frac{\nu}{2\pi}\int_\alpha^\beta \sqrt{\frac{\beta - x}{x - \alpha}} \log\left(\frac{x-\alpha}{x}\right) dx$$

$$J_3 = -2\pi \int_\alpha^\beta \sqrt{\frac{\beta - x}{x - \alpha}} \nu(x)dx \qquad J_4 = \int_\alpha^\beta \sqrt{\frac{x-\alpha}{\beta - x}} S^2(x)dx$$

$$J_5 = \frac{\nu}{2\pi}\int_\alpha^\beta \sqrt{\frac{x-\alpha}{\beta - x}} \log\left(\frac{x-\alpha}{x}\right) dx \qquad J_6 = -2\pi \int_\alpha^\beta \sqrt{\frac{x-\alpha}{\beta - x}} \nu(x)dx$$

If we suppose for the moment that $\nu(x)$ is known, it is now possible to set up an iterative solution scheme using (9). For simplicity, we assume that the region [0,1] is divided into N equally spaced intervals of width dx and that $\alpha = n_\alpha dx$ and $\beta = n_\beta dx$ where $0 < n_\alpha < n_\beta < N$. Approximating S as being a piecewise constant on each interval (higher order approximations are also possible, but acceptable accuracy was achieved with this simple scheme), we assume that a previous iterate $S^{(n)}(x)$ is known. Values for Γ^2 and λ are calculated from the expressions (10) and (11) and colocation is used to produce values for $S^{(j+1)}(x)$ at mesh points $x_n = ndx$, where $n_\alpha < n < n_\beta$ via the formula

$$S^{(j+1)}(x_n) = -\frac{2}{\pi}\mathrm{Sin}^{-1}\sqrt{\frac{\beta - x_n}{\beta - \alpha}} \sum_{i=1}^{4} K_i + \frac{1}{\pi}\sum_{i=5}^{8} K_i(x_n) \qquad (12)$$

where

$$K_1 = \lambda\pi(\alpha - \beta) \qquad K_2 = \frac{\Gamma^2}{4}\int_\alpha^\beta (S^{(j)}(t))^2 dt$$

$$K_3 = \frac{\nu}{\pi}\int_\alpha^\beta f_1(t) \log\left(\frac{t-\alpha}{t}\right) dt \qquad K_4 = -4\pi \int_\alpha^\beta f_1(t)\nu(t)dt$$

$$K_5(x_n) = -\int_\alpha^\beta 2\lambda f_2(x_n, t)dt \qquad K_6(x_n, t) = \frac{\Gamma^2}{4}\int_\alpha^\beta (S^{(j)}(t))^2 f_2(x_n, t)dt$$

$$K_7(x_n) = \frac{\nu}{\pi}\int_\alpha^\beta \log\left(\frac{t-\alpha}{t}\right) f_2(x_n, t)dt \qquad K_8(x_n) = -4\pi \int_\alpha^\beta \nu(t) f_2(x_n, t)dt$$

and

$$f_1(t) = \sqrt{\frac{t-\alpha}{\beta - t}}$$

$$f_2(x,t) = \log\left(\frac{\left(\sqrt{(\beta - t)(x-\alpha)} + \sqrt{(\beta - x)(t-\alpha)}\right)^2}{(\beta-\alpha)|x-t|} \right)$$

Given piecewise constant values for S and ν there are many ways of approximating the integrals, but since the method is an iterative one and there are likely to be many integral evaluations, the simple trapezium rule was used for integrals involving S and ν, whilst a general-purpose NAG routine was used for J_2, J_5, K_5 and K_7. The scheme (12) assumes that the function $\nu(x)$ is known, but in reality it has to be calculated at each iteration using the previous iterate for S. There are a number of different methods which could be employed to calculate ν via (7) One approach which avoids the use of derivatives involves integrating (7) to give the Fredholm equation

$$\int_0^1 \nu(t) \log\left(\frac{x-t}{1-t}\right) dt = \frac{\mu}{2}(1-x) - \frac{S(x)}{4} \qquad (13)$$

The advantage that no derivatives are present is heavily outweighed, however, by the fact that this is a Fredholm equation of the first kind, and we may anticipate ill-conditioning problems These fears are borne out in practice, and, though for a small number of mesh points simple methods produce an adequate solution, the accuracy for finer meshes is not acceptable As an alternative to this unsatisfactory method, equation (7) may be inverted to yield

$$\nu(x) = -\frac{\mu}{2\pi}\sqrt{\frac{1-x}{x}} - \frac{1}{4\pi^2}\sqrt{\frac{1-x}{x}} \int_0^1 \sqrt{\frac{t}{1-t}} \frac{S'(t)dt}{t-x} \qquad (14)$$

and, since S is given for $0 \le x \le \alpha$ and $\beta \le x \le 1$, to evaluate ν we need only approximate $S'(x)$ in $[\alpha, \beta]$. Various methods are available for this, but using a simple central difference combined with mid-point evaluation of the singular integral leads to the formula

$$\nu_k = \frac{\nu_{k+\frac{1}{2}} + \nu_{k-\frac{1}{2}}}{2}$$

where

$$\nu_{k+\frac{1}{2}} = -\frac{\mu}{2\pi}\sqrt{\frac{1 - x_{k+\frac{1}{2}}}{x_{k+\frac{1}{2}}}} - \frac{1}{4\pi^2}\sqrt{\frac{1 - x_{k+\frac{1}{2}}}{x_{k+\frac{1}{2}}}} \int_0^1 \sqrt{\frac{1}{1-t}} \frac{\bar{S}'(t)dt}{t - x_{k+\frac{1}{2}}}$$

with

$$\bar{S}'(x) = \frac{S_{k+1} - S_k}{dx}$$

for $x_k < x < x_{k+1}$

This crude method is surprisingly accurate and, although higher order methods could be employed, provides quite acceptable accuracy The method is implemented by making an initial "guess" for $S^{(0)}(x)$, and then calculating initial estimates for ν, Γ^2 and λ. Experiments showed that the scheme was insensitive to choice of $S^{(0)}(x)$, but in all the calculations reported below the choice

$$S^{(0)}(x)=\frac{\nu(x-\beta)^2[x(\alpha+\beta)-2\alpha^2]}{(\beta-\alpha)^3}$$

was employed so that the correct derivative conditions are satisfied. The initial estimates for ν, Γ^2 and λ are then used in (12) to predict $S^{(1)}(x)$, and the scheme may continue. In practice, it was found that convergence was satisfactory, with three decimal-place accuracy being produced in about 20 iterations. The results of (2), which correspond to the case $\mu = 0$, $\nu = 0$ provided a partial check for the method.

RESULTS AND CONCLUSIONS

Once the numerical method has converged, it is possible to calculate the lift L_a. Note that the pressure is symmetric about the centreline of the cavity and so the pressure on the top surface of the cavity is identical to the pressure on the bottom surface of the cavity (the top surface of the aerofoil). Thus the lift on the aerofoil is the same as the lift on the aerofoil/cavity combination, which is given by

$$L_a=\rho U_\infty\int_0^1 \nu(x)\mathrm{d}x$$

The non-dimensional lift

$$C_L=\frac{L_a}{\rho U_\infty}$$

is thus calculated by a simple numerical integration. Results for a number of cases are shown in Figs 2, 3 and 4. In each case the number of computational points was determined by the requirement that three-figure accuracy should be produced. In Fig. 2 the value $\mu = 0$ was used and $\nu(x)$ was artificially forced to be identically zero The values α = 1/6, β = 5/6 and $\nu = 2\pi$ were taken, and

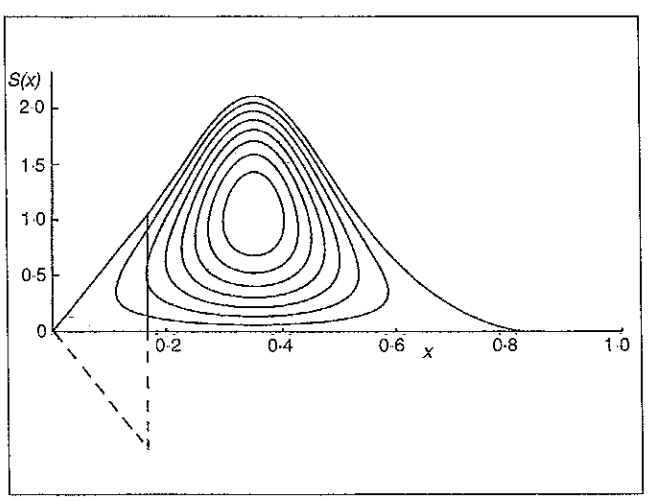

Figure 2. Symmetrical (Childress) case when $\nu(x)$ is forced to be zero ($\mu = 0$, $\nu = 2\pi$)

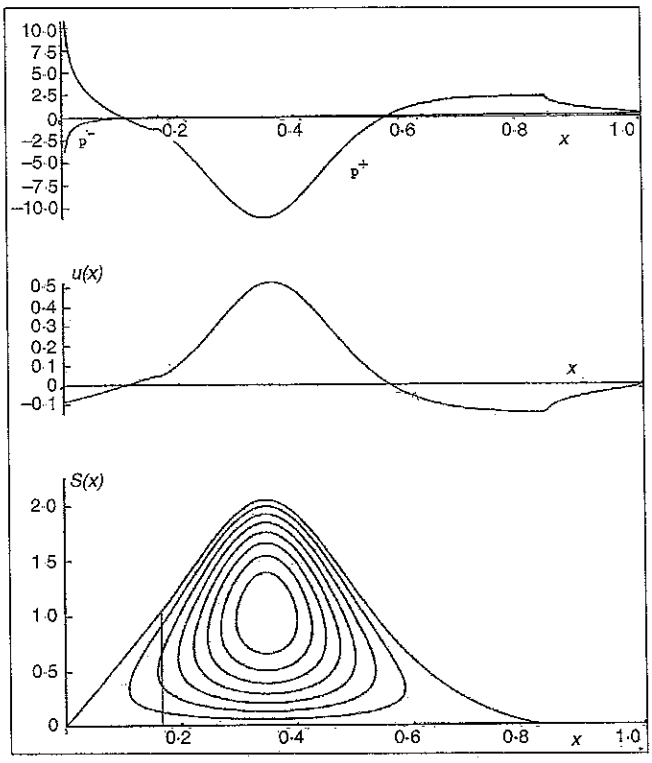

Figure 3a. Pressures, $u(x)$ and cavity shape for case $\mu = 0$, $\nu = 2\pi$ with β = 5/6 (C_L = 0·1161)

192 points were used. This case therefore corresponds to one of the flows considered in Section 2, and it may be easily verified that the results match those reported in that study In this case the flow is symmetrical and consequently the lift is zero. The final values of λ and Γ^2 were respectively 1·283 and 12·521. The cavity shape and the streamlines within the cavity are shown. Note that, as in all the examples that will be considered, the streamlines have been continued into the wedge in front of the cavity. In reality, of course, the streamlines cannot intersect this solid boundary but must be contained entirely within the cavity This problem may be surmounted by considering a further inner region where the flow is fully two-dimensional; it was indicated in Section 2 how such an analysis could be performed. In Fig 3a the non symmetrical version of the Childress problem has been solved, where the angle of incidence is still zero but $\nu(x)$ is now not forced to be zero.

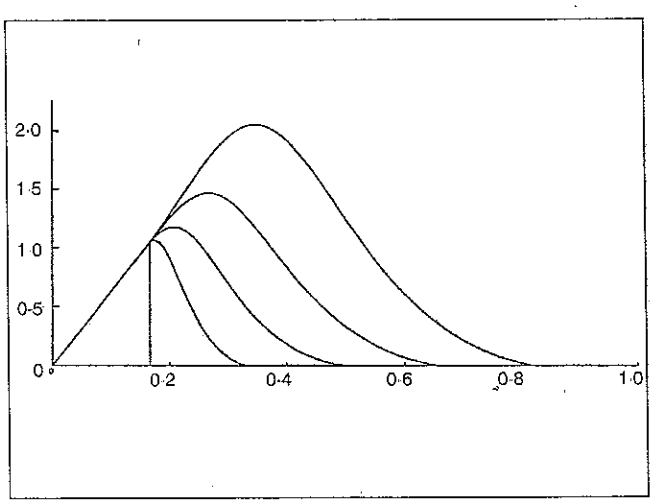

Figure 3b Cavity shapes for various β for case $\mu = 0$, $\nu = 2\pi$.

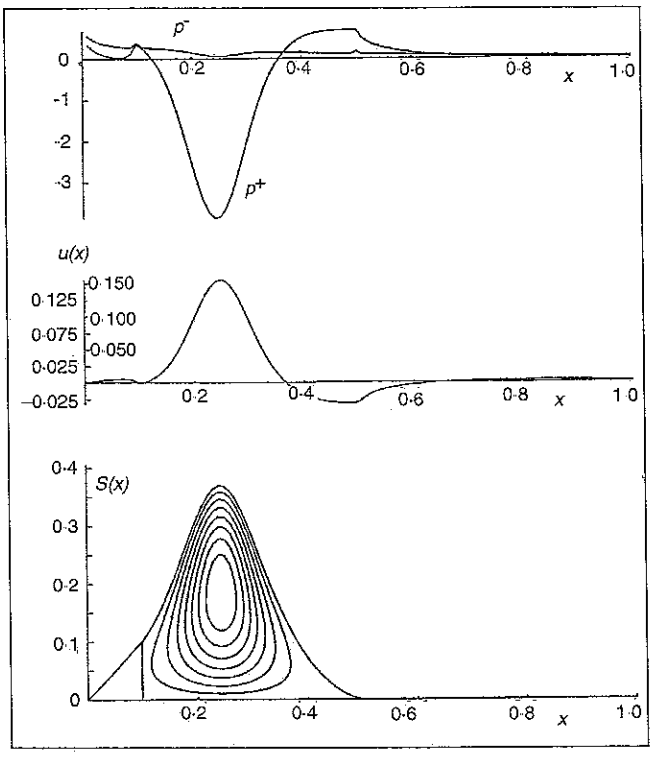

Figure 4. Pressures, $u(x)$ and cavity shape for case $\mu = 0{\cdot}1$, $\nu = 1$ with $\alpha = 1/10$, $\beta = 1/2$ ($C_L = 0{\cdot}03502$).

Again the values $\alpha = 1/6$, $\beta = 5/6$ and $\nu = 2\pi$ were taken, and 192 points were used. The lift coefficient C_L in this case was 0·1161. The bottom part of the figure shows the cavity shape and the streamlines, and above this values of $u(x) = v(x)x^{1/2}$ are shown. At the top of the figure, the perturbation pressures p^+ and p^- on either side above and below the aerofoil/eddy combination, defined by

$$p^{\pm} = -\frac{1}{2\pi}\int_0^{\beta} \frac{S'(t)}{x-t}\,dt \mp 2\pi v(x)$$

where the non-dimensional pressure is

$$p = \frac{p_\infty}{\rho U_\infty^2} + \varepsilon p^{\pm}$$

are plotted. In Fig. 3b the effect of variations in the reattachment point β is examined. Again 192 points were used for each of the computations and the values $\alpha = 1/6$, $\nu = 2\pi$ and $\mu = 0$ were used. Cavity shapes are shown for the values $\beta = 5/6$, 2/3, 1/2 and 1/3, the values of the associated lift coefficient C_L being given respectively by 0·1161, 0·0614, 0·0362 and 0·0224. As expected, the lift decreases with decreasing β.

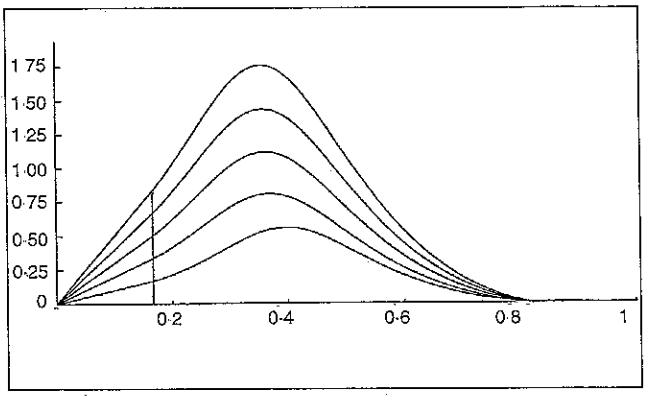

Figure 5. Cavity shapes for various spoiler heights ($\mu = -0{\cdot}1$)

Figure 4 shows results for a case where the angle of incidence is non-zero. The values $\alpha = 1/10$, $\beta = 1/2$, $\mu = -0{\cdot}1$ and $\nu = 1$ were used and a calculation with 100 points showed that the lift was given by $C_L = 0{\cdot}03502$ whilst λ and Γ^2 were given respectively by 0·7003 and 268·7. One obvious conclusion for case where the angle of incidence is non-zero is that the lift depends linearly on μ. Indeed, μ may be scaled out of the problem. In Fig. 5, the effect of varying the spoiler height is examined. Cavity shapes are shown for the values $\alpha = 1/6$, $\beta = 5/6$, $\mu = -0{\cdot}1$. The calculations were performed with 192 points and $\nu = 1(1)5$. The respective lift coefficients for the five cases were 0·055178, 0·069716, 0·087313, 0·10541 and 0·12367 showing that, though the lift increases with spoiler height the relationship is not a linear one. It should be noted that comparisons between large and small spoiler sizes must be treated with caution, as the unknown vorticity in the Prandtl-Batchelor region may change from case to case.

REFERENCES

1 BATCHELOR, G.K. On steady laminar flow with closed streamlines at large Reynolds number, *J Fluid Mech*, 1956, **1**, pp 177-190

2. CHILDRESS, S. Solutions of Euler's equations containing finite eddies, *Phys Fluids*, 1966, **9**, pp 860-872

3 O'MALLEY, K., FITT, A.D., JONES, T.V., OCKENDON, J.R. and WILMOTT, P. Models of high-Reynolds-number flow down a step, *J Fluid Mech*, 1991, **222**, pp 139-155.

4. WOODS, L.C. *The Theory of Subsonic Plane Flow*, Cambridge University Press, 1961.

5 OCKENDON, H. and TAYLER, A.B *Inviscid Fluid Flow*, Springer-Verlag, 1983